1st International Conference on Sensing Technology
November 21-23, 2005 Palmerston North, New Zealand

Analysis of document authentication technique using magneto-resistance sensor detecting soft magnetic fibers

Ayumi Aoki, Takashi Ikeda, Tsutomu Yamada, Yasushi Takemura* and Tsutomu Matsumoto
Yokohama National University, Japan
*e-mail: takemura@ynu.ac.jp

Abstract

An artifact-metric system using magneto-resistance (MR) sensor detecting magnetic fibers can be applied for authentications of stock certificate, bill, passport, plastic cards and other documents. The security of the system is guaranteed by its feature of difficulty in copy or reproduction. This authentication system is based on the soft magnetic fibers dispersed randomly in the documents. The modeling of the dispersed magnetic fibers and the calculation of detected signals by the MR sensor have been performed. By calculating the output waveform of the MR sensor, a false match rate (FMR) was analyzed. Optimizations of the density of the magnetic fibers and the dimension of the MR sensor were achieved.

Keywords: authentication system, artifact-metrics, magnetic fiber, magneto-resistance (MR) sensor

1 Introduction

A personal authentication using a biometrics has been widely used. The biometrics utilizes individually intrinsic features of the human body such as fingerprint, retina and face. It is normally difficult to copy these unique features or modify them intentionally. The advantages of the biometrics can be similarly realized for the authentication of stock certificate, bill, passport, plastic cards and other documents by supplying randomly determined characteristics. It has been reported that the documents with randomly dispersed magnetic fibers can be used for authentication classified as artifact-metric system [1]. The security of the system is guaranteed by difficulty in reproducing or copying the intrinsic distribution of the magnetic fibers. In order to evaluate this authentication technique, modeling of the randomly dispersed magnetic fibers and detected signals from a magneto-resistance (MR) sensor is performed in this study. A false match rate is analyzed as an evaluation the authentication accuracy of this system.

2 Artifact-metric system

Magnetic stripe cards such as cash card and credit card have series of magnets whose magnetization directions denote one-bit information of 0 or 1 as shown in Fig. 1a. As the signal waveform detected by a magnetic sensor is simple, it is easy to determine the distribution of the magnetic stripe pattern from the signal waveform.

Figure 1b shows an example of the pattern of randomly dispersed magnetic fibers. The signal waveform obtained from this pattern is more complicated.

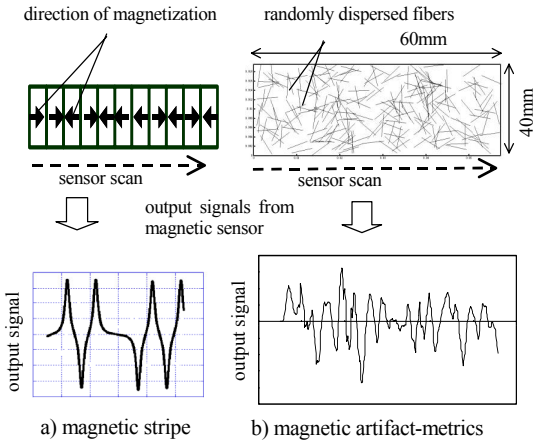

Figure 1: Comparison of authentication techniques using magnetic stripe (a) and a magnetic artifact-metric system (b).

It is difficult to determine the distribution of the random positions of the fibers from the signal waveform, which is a unique feature of the artifact-metric system.

3 Model of artifact-metric system

3.1 Document with randomly dispersed magnetic fibers

In order to evaluate the authentication accuracy of the artifact-metric system using the magnetic fibers, a sheet of document embedded randomly dispersed

magnetic fibers was assumed. The size of the document was 60mm×40mm. The positions (distributions) of the magnetic fibers were decided by a conventional function of random number generator. The magnetic fiber was 5 mm length in straight shape. The density of the fiber was varied from 2 to 200 cm^{-2}. Figure 1b shows the example of the document with the magnetic fibers of 20 cm^{-2}.

3.2 MR sensor and output waveform

The output signal obtained from the document by using a differential type MR sensor was calculated. The MR sensor consisted of two elements of MR sensor (indicated as MR_1 and MR_2 in the figure) and a permanent magnet for biasing the MR sensor.

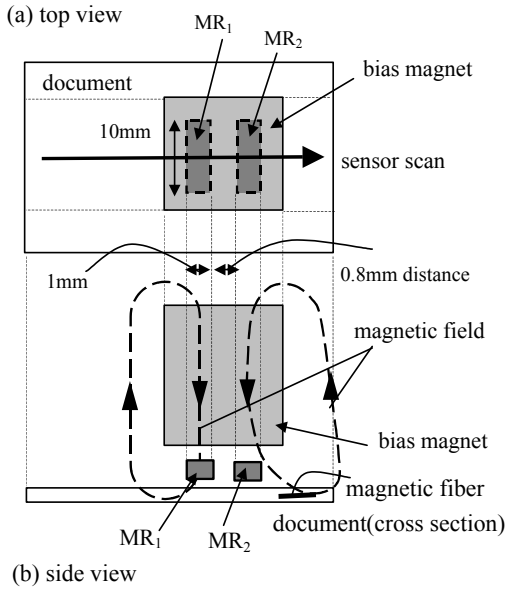

Figure 2: Detection of soft magnetic fibers with differential-type MR sensor. Top view (a) and side view (b).

Figure 2a and 2b show its top view and size view, respectively. The size of both sensor elements was 1 mm× 10 mm, and they were placed in a distance of 0.8 mm as shown by the top view of Fig. 2a. Symmetric magnetic field was applied to the sensor elements by the bias magnet. When the magnetic fiber is passing under the MR sensor, the distribution of the magnetic flux changes as to increase the flux density in the magnetic fiber. As a result, the magnetic flux density applied to the sensor elements becomes asymmetric between them as shown in the cross-sectional view of Fig. 2b.

When the magnetic fiber is passing under MR_1 (MR_2) as shown in Fig.3a (3c), the applied magnetic field to MR_1 (MR_2) is larger than that to MR_2 (MR_1). In case that the magnetic fiber is located at the middle position between MR_1 and MR_2 as shown in Fig. 3b, the applied magnetic field to MR_1 and MR_2 is symmetric.

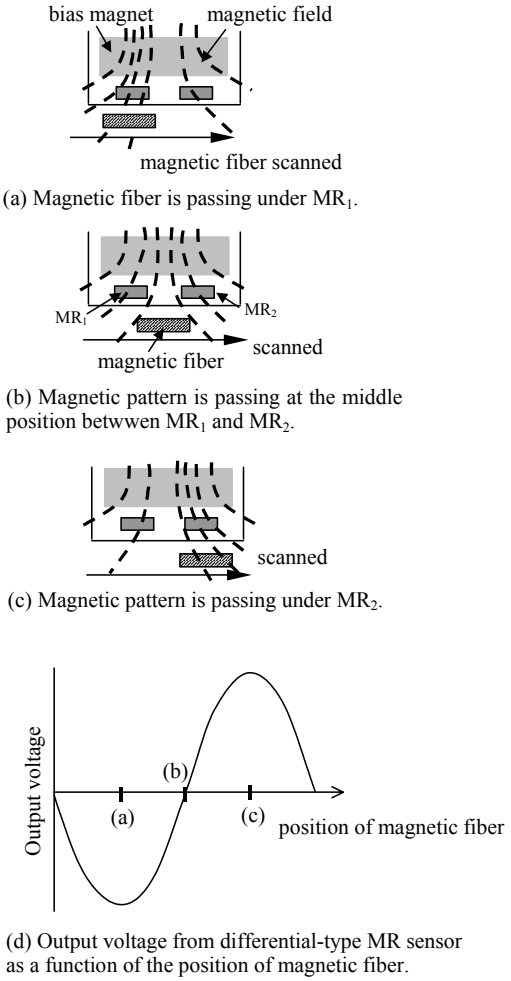

Figure 3: Detection of the magnetic fiber using the differential-type MR sensor. The spatial distribution of magnetic flux density changes when the magnetic fiber is passing under the MR sensor as indicated in (a), (b) and (c). The output voltage of the sensor is also shown in (d).

The equivalent electric circuit of the differential type MR sensor is illustrated in Fig. 4.

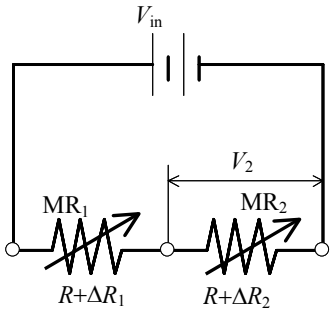

Figure 4: Circuit for differential-type MR sensor.

In case that no magnetic materials exist near the sensor, the elements of MR_1 and MR_2 have equivalent resistance of R as an initial resistance value. The

resistance R of each element changes in accordance with the applied magnetic field due to magnetoresistance effect. In this analysis, the resistance change of each element, ΔR_1 or ΔR_2, is assumed to be proportional to the amount of fibers covered by each element. The voltage across MR_2 is described as:

$$V_2 = \frac{R + \nabla R_2}{R + \nabla R_1 + R + \nabla R_2} \times V_{in}, \quad (1)$$

where V_{in} is a constant dc voltage applied to the series connection of MR_1 and MR_2 as shown in Fig. 4. As the resistance change of the MR sensor element is several %, it can be assumed that $R >> \Delta R_1$ and $R >> \Delta R_2$. Then the output voltage V_{out} is calculated as:

$$\begin{aligned} V_{out} &= V_2 - \frac{1}{2} V_{in} \\ &= \frac{R + \Delta R_2}{R + \Delta R_1 + R + \Delta R_2} \times V_{in} - \frac{1}{2} V_{in} \\ &= \frac{\Delta R_2 - \Delta R_1}{2(R + \Delta R_1 + R + \Delta R_2)} \times V_{in} \\ &\approx \frac{\Delta R_2 - \Delta R_1}{4R} \times V_{in} \\ &\propto (\Delta R_2 - \Delta R_1). \end{aligned} \quad (2)$$

From this equation, it is found that the output voltage V_{out} is approximately proportional to the difference in the resistance change of MR_1 and MR_2. Figure 3d shows the output voltage during the magnetic fiber passing under the MR sensor sensor as indicated by Fig.3a-3c.

4 Evaluation of authentication

4.1 Verification between template and sample patterns

In order to evaluate the authentication accuracy of the documents, the signal waveform obtained from the MR sensor was analyzed. A template pattern is defined as a specific output waveform recorded from a genuine document. This pattern is in the custody of any storage devices and used for the authentication of documents by comparing the detected waveform from other documents. At first, the template pattern was determined by calculating the specific distribution of the magnetic fibers by the random number generator. Next, 10^8 individual patterns were determined also by the random number generator. These patterns, defined as sample patterns, were presumed to be different distribution of the magnetic fibers. The template pattern and one of the sample patterns were compared and deicide if they were authenticated as same or equivalent documents.

4.2 Calculation of similarity

A degree of similarity between the template and sample patterns was calculated. The waveform of each pattern was obtained by scanning the MR sensor along the document for 50 mm as shown in Fig. 5a. The output voltage V_2 was measured every 0.1 mm of the sensor scan and its waveform was obtained as shown in Fig. 5b.

The template and sample waveforms are described as

$$P = (p_1, p_2, \cdots, p_{500}) \quad (3)$$

$$Q = (q_1, q_2, \cdots, q_{500}) \quad (4)$$

where p_i and q_i are the detected voltages of V_2, for template and sample patterns, respectively.

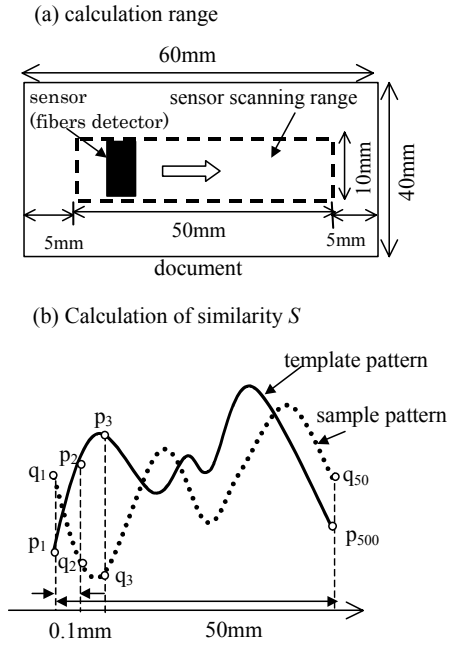

Figure 5: Calculation of similarity S. Calculation range(a) and how to take the data from template pattern and sample pattern(b).

Then the degree of similarity between template waveform P and sample waveform Q, defined as $S(P,Q)$, was calculated by the following equation:

$$S(P,Q) = \frac{\sum_{i=0}^{500} (p_i - \bar{p}) \cdot (q_i - \bar{q})}{\sqrt{\sum_{i=0}^{500} (p_i - \bar{p})^2 \cdot \sum_{i=0}^{500} (q_i - \bar{q})^2}} \quad (5)$$

where $\bar{p}$ and $\bar{q}$ are mean values of all the elements of P and Q, respectively. The similarity S is in the range of $-1 < S < 1$. The higher value of S is obtained from similar waveforms of P and Q. A threshold value for the similarity S_t was defined in order to decide if two waveforms were obtained from the same or equivalent pattern.

4.3 Evaluation by False Match Rate

False Match Rate (FMR) is a probability that the artifact-metric system incorrectly accepts the false documents in authentication process. This FMR is used for the evaluation of the authentication technique using the magnetic fibers. The lower FMR value indicates the higher performance of the authentication system.

The each of 10^8 sample documents was determined if it was accepted or not as the genuine document by calculating the similarity S between the template pattern and each sample pattern. From this FMR analysis, a number of patterns that were recognized as different from each other could be evaluated. In this study, the optimization of the fiber density and the dimension of the MR sensor were reported.

5 Analytical results

5.1 Fiber density dependence of FMR

Figure 6 shows a calculated result of the FMR indicated as a function of the density of the magnetic fibers embedded in the documents. The FMR was calculated for using various threshold value of S_t from 0.5 to 0.8. It is obvious that the higher value S_t can reduce the FMR, indicating the high similarity is required for accepted as a genuine pattern. It is also found that the FMR has its minimum value of 10^{-6} at around the fiber density of $20cm^{-2}$.

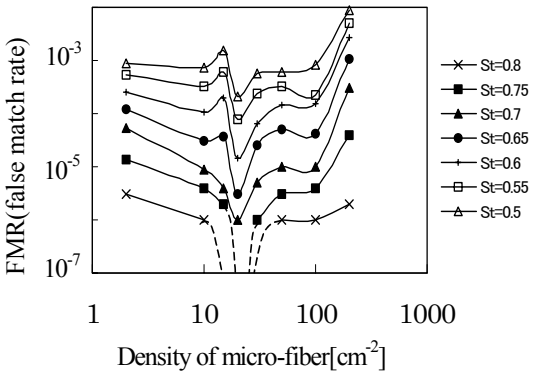

Figure 6: FMR indicated as a function of fiber density for various threshold *S*t.

The examples of the patterns and their detected signal waveforms for the fiber densities of $2cm^{-2}$, $20cm^{-2}$ and $200cm^{-2}$ are shown in Fig. 7. In case of $2cm^{-2}$, the number of the fiber is quite low, and the waveform is simple. When the fiber density is $20cm^{-2}$, the waveform becomes more complicated in accordance with the number of the fibers. But the waveform becomes simple and its amplitude, detected voltage of V_2 discussed in section 3.2, is lower for the $200cm^{-2}$ case. It is because that that the difference in the number of fibers covered by MR_1 and MR_2 is not large for a large amount of fibers. From this analysis, it is estimated that the fiber density of is $20cm^{-2}$ is a optimum condition.

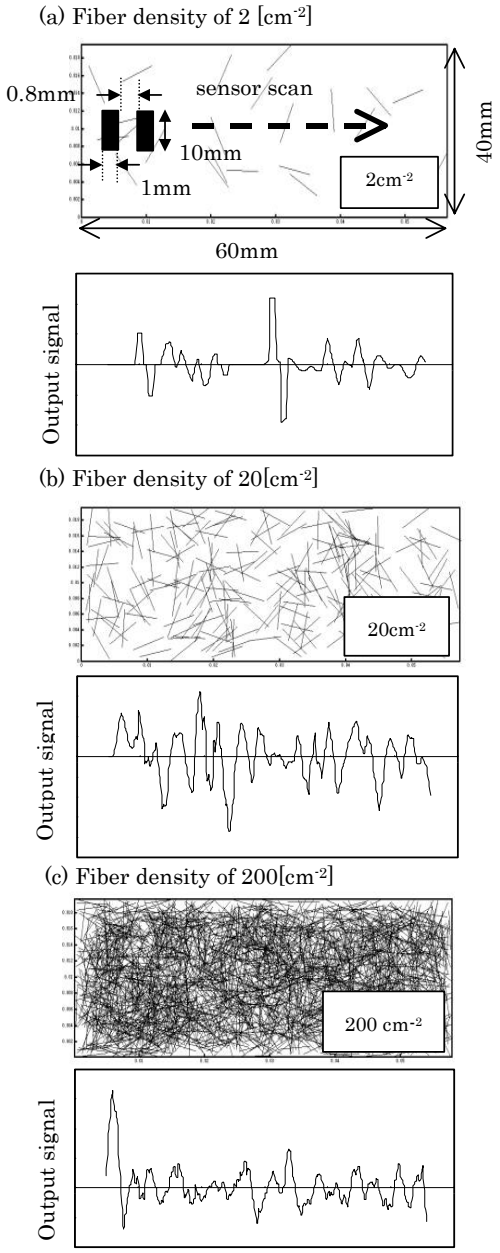

Figure 7: Schematics of patterns and signal waveforms for fiber density of (a) 2 cm^{-2}, (b) 20 cm^{-2} and (c) 200 cm^{-2}.

5.2 Sensor size dependence of FMR

The FMR value was also dependent on the dimension of the MR sensor. Figure 8 indicates the calculated FMR values as a function of the fiber density. The dimension of the sensor element was varied from 0.1mm×1mm to 2mm× 20mm. The aspect ratio of 1:10 for their dimension and the distance between two elements of 0.8 mm were constant. The threshold value of S_t=0.65 was used.

The FMR was not below 10^{-3} at any fiber density, which suggests that the sensor size was not suitable.

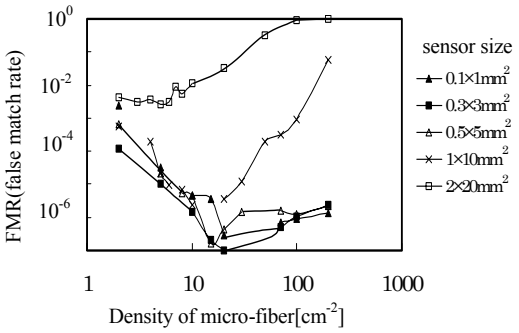

Figure 8: FMR as a function of dimension of MR sensor

The sensor size of 1mm× 10mm gives the lowest FMR around 10^{-6} at the fiber density of is 20cm^{-2}. For the smaller sensor size than 20cm^{-2}, the FMR was not changed much including its fiber density dependence. It can be concluded that the sensor dimension should be 1mm× 10mm or smaller.

6 Conclusions

In this paper, the accuracy of authentication of artifact metric system using soft magnetic fibers is evaluated. The analytical modeling of the randomly dispersed magnetic fiber and the magnetoresistance sensor was proposed. The false match ratio, FMR was calculated in order to optimize the fiber density and sensor dimension. It has been demonstrated that the artifact-metric system using the magnetic fiber provides the authentication accuracy of the FMR of as low as 10^{-6}.

As it normally takes a long time and much cost to evaluate the accuracy of authentication system, the numerical analysis proposed in this study is advantageous.

7 Acknowledgements

The authors acknowledge Information and Security Systems Division, NHK SPRING CO., LTD., Japan for valuable discussions.

8 References

[1] Matsumoto, H. and Matsumoto, T., "An Evaluation Method for a Magnetic Artifact-metric System", *IPSJ Journal*, Vol.43, pp 2458-2466 (2002).